Robertson, A.H.F., Emeis, K.-C., Richter, C., and Camerlenghi, A. (Eds.), 1998
Proceedings of the Ocean Drilling Program, Scientific Results, Vol. 160

42. ACOUSTIC PROPERTIES FROM LOGS AND DISCRETE MEASUREMENTS (SITES 966 AND 967) ON ERATOSTHENES SEAMOUNT: CONTROLS AND GROUND TRUTH[1]

John M. Woodside,[2] Jeroen A.M. Kenter,[2] and Ad Köhnen[2]

ABSTRACT

Acoustic properties (*P*-wave velocities, densities, and porosities) and insoluble residues were measured at in situ pressures in 68 core plugs taken from cores recovered at Ocean Drilling Project Sites 966 and 967 and compared with wireline logging data. Study of the parameters that control the acoustic properties and the quality of the logging data reveals: (1) velocity-porosity and velocity-density relationships within the discrete data follow the general trend of the general empirical equation but are offset with respect to it. Insoluble residue and dolomite content are the primary controls on the acoustic velocities of the core plugs, whereas lithologic facies has no or a minor effect; and (2) velocity-porosity and velocity-density relationships in the logging data show considerable deviation and trends that cross those from the general relationships that are believed to approximate fundamental physical principles. Calculated uncertainties in the laboratory measurements are at least one order of magnitude smaller than the difference between laboratory measurements and those from the wireline logs in several intervals. As a consequence, we believe that the downhole wireline measurements are unreliable in large intervals at both sites. Possible causes of the unreliability are poor hole conditions, upscaling effects, and consequent difficulties in making realistic corrections of the raw log data. The wireline logs were found to be of such poor quality that they are untrustworthy sources of acoustic parameters for making synthetic seismograms. This study clearly indicates that logging data should be carefully evaluated and calibrated with petrophysical relationships from literature and from discrete measurements before interpretation or use as input for synthetic seismograms when hole conditions are poor.

INTRODUCTION

One of the objectives of Ocean Drilling Project (ODP) Leg 160 drilling was to provide a means of calibrating seismic reflection data from Eratosthenes Seamount, and perhaps the region around it, by obtaining ground truth petrophysical data. The physical causes of seismic reflectors are dependent primarily on contrasts in the acoustic velocity and density of rocks and sediments with depth, and secondarily on both the geometry of interfaces separating units with distinct acoustic properties and gradients and inhomogeneities in these properties. Furthermore, it is known that shipboard and downhole wireline measurements may not always provide reliable estimates of in situ acoustic velocities, porosities, and densities (e.g., Paillet and Cheng, 1991; Theys, 1991; Kenter and Ivanov, 1995). Therefore, this study was undertaken to make such measurements and to use them (a) to find the parameters controlling the acoustic properties, (b) to examine deviations between logging and laboratory measurements and address the quality of these data, and (c) to use the data obtained in the creation of synthetic seismograms that could be compared directly with the site survey seismic reflection profiles. Goal (c) is not addressed in this paper. The ultimate goal is to understand the seismic response of the geology.

A secondary aim of this paper is to shed a little light on the use of wireline logging information in scientific research as carried out within ODP. To paraphrase Theys (1991) in the preface to his book, because wireline logging has been seen by some to be an esoteric art shrouded in some mystery because of the paucity of information about it, little attention has been given to the underlying physical processes and the meaning and relevance of the wireline data. We feel that this is especially true in the case of ODP, where drilling conditions are often difficult and the scientific requirements of the logs can be quite different than those used in the exploration industry where logging was developed. We need to address the problems of logging quality and the underlying petrophysical influences of logging variability.

The Eratosthenes Seamount is a major topographic feature in the eastern Mediterranean. It is a slightly north-northeast–south-southwest elongated block of about 100 × 70 km that rises over 1200 m from the seafloor ~100 km south of Cyprus (Emeis, Robertson, et al., 1996). Site 966 is located on the northern margin of the plateau area of the Eratosthenes Seamount in a water depth of 940 m. Site 967 is located on a small ridge trending west-southwest to east-northeast at the base of the northern slope of the Eratosthenes Seamount in water 2554 m deep. The samples from Holes 966F and 967E consist of carbonate rocks, some pure but most with small admixtures of clay.

Little information is available on the acoustic behavior of carbonates. Several studies have been made (e.g., Rafavich et al. 1984; Anselmetti and Eberli, 1993; Kenter and Ivanov, 1995; Kenter et al., 1997a, 1997b) that show the primary factors controlling acoustic velocity in nearly pure carbonates are both the amount and type of porosity, diagenetic properties, and mineralogy. The classic velocity transforms, Wyllie's time-average equation (Wyllie et al., 1958) and Gardner's empirical relation (Gardner et al., 1974), can predict *P*-wave velocity from porosity or bulk density in single data sets, but fail to account for the variation in velocity at a given porosity value. For carbonates in general, such empirical relationships have big limitations because they do not take into account the type of porosity, diagenetic parameters or mixed mineralogy (e.g., Anselmetti and Eberli, 1993; Kenter et al., 1997a). In general, the empirical equations for carbonates do not satisfactorily explain much of the variation observed in discrete data sets. Trends in most published data, however, follow the time average and Gardner et al.'s (1974) equation. It is thus accepted that the latter two relationships represent fundamental physical principles in the elastic behavior of sedimentary rocks (Bourbié et al., 1987). As such, even though extrinsic parameters like pressure and temperature are different, velocity-porosity and velocity-density relationships in log data should obey general trends observed in the empirical relationships (Theys, 1991).

[1]Robertson, A.H.F., Emeis, K.-C., Richter, C., and Camerlenghi, A. (Eds.), 1998. *Proc. ODP, Sci. Results*, 160: College Station, TX (Ocean Drilling Program).

[2]Department of Earth Sciences, Vrije Universiteit, De Boelelaan 1085, 1081 HV Amsterdam, The Netherlands. Woodside: wooj@geo.vu.nl

Prior Chapter Contents Next Chapter

In this paper, we report on the controls of the acoustic properties of the nearly pure carbonates recovered from Holes 966E and 967F. In addition, we compare and evaluate the variations in velocity, density, and porosity between the discrete data set and the wireline logging data. Our main objective is to assess the reliability and quality of the wireline logging data when used for synthetic seismograms to aid in correlating the rock record with seismic reflection data.

METHODS

Although sufficient for our purposes, the sampling was not ideal because of poor core recovery. Recovery for Holes 966F and 967E was 22.1% and 14.8%, respectively. Sixty-eight minicores (or core plugs of 2.54 cm in diameter and of similar length) were taken from these cores. The downhole representation of physical properties by the samples is limited by (a) the possibly poorly representative recovery, and (b) the limited sampling within the recovered sections. Furthermore, the samples are not evenly distributed over the depth range because of bad recovery from several depth intervals. The minicores were stored in plastic containers filled with seawater from the cores. Twenty-four samples were taken from Hole 966F between 125 and 350 mbsf, and 43 samples from Hole 967E between 130 and 410 mbsf. One sample from Hole 967A is included because it was very close to Hole 967E. Fifty-nine samples were oriented vertically and nine horizontally to check for anisotropy in the direction of measurements.

Measurements of sonic velocity under in situ pressure conditions and other petrophysical properties (bulk density, grain density, and porosity) were made on the 68 2.54-cm-diameter core plugs. Thin sections were made from all samples for petrographic observations to classify the samples by rock fabric and by type of porosity. The physical properties measurements were combined with values of carbonate content and X-ray fluorescence spectroscopy (XRF) observations to determine the mineralogic composition of the samples. In the laboratory, the core plugs were removed from their seawater immersion and stored in a seawater equivalent under vacuum for a period of 72 hr to ensure that they were saturated with brine.

The experimental procedure for obtaining the acoustic velocities involves measuring the one-way travel time along the sample axis and dividing by the sample length. In the experiment, a source and receiver pair of similar crystals are selected through an ultrasonic signal selector switch. The source crystal is excited by a fast rise time electrical voltage pulse, which produces a broadband ultrasonic pulse with frequencies between 300 and 800 kHz. The arrival time is picked when the signal exceeds a threshold voltage equal to 3% of the overall peak-to-peak amplitude of the first three half-cycles of the signal. Precision of the velocity measurement in low-porosity carbonates is within approximately 0.5%. The ultrasonic measurements were conducted at effective pressures ranging from 2 to 40 MPa in confining/pore pressure combinations of 2/0, 6/2, 12/4, 21/7, 45/15, and 60/20 and back in the same steps to 6/2 MPa; however, the values reported here were all from measurements made at 12/4 MPa with an effective pressure of 8 MPa.

Following the measurement of the acoustic velocities, saturated sample mass and sample volume were measured with the assumption that the samples were perfectly cylindrical (within the estimated error of ≤0.1% and ≤2% respectively, including possible "rebound" effects associated with the reduced pressure at the return to laboratory conditions). Subsequently, the samples were dried for 72 hr at 70°C. The dry mass of the samples was measured, and the wet-bulk and dry-bulk densities (ρ_b and ρ_d) calculated from the saturated and dry mass, and volume, respectively, each with an estimated possible error of ≤2%. From each sample, subsamples were taken for the measurements of grain density and carbonate content. Grain density (ρ_g) was calculated to better than 1% from the mass and volume of the powder, measured with a helium pycnometer. Total porosity (ϕ) was calculated (estimated error of 3%) from the grain density and dry density (ρ_g and ρ_d). Table 1 summarizes the petrophysical measurements for Sites 966F and 967E, respectively.

X-ray fluorescence spectroscopy was used to define the weight percentages of the predominant minerals. In 25 selected samples that represent the different lithologies, the weight percentages of dolomite and calcite in the samples were calculated from the partitioning of dolomite and calcium carbonate as determined from the XRF data. All the MgO present in the samples was assumed to be contributed by dolomite. The selected samples containing high weight percentages of MgO do not contain relevant amounts of SiO_2 and Al_2O_3, thus excluding the presence of clay minerals that would be the other most likely contributor of MgO. We can not exclude, however, the presence of clay minerals in the remaining samples. The amount of CaO and MgO needed for the precipitation of dolomite was calculated using an MgO:CaO ratio of 10:8 (Reeder, 1983). After subtracting the CaO calculated for the dolomite from the total amount of CaO, the remaining CaO was assumed to be entirely from calcium carbonate. Dolomite content in 100% carbonate samples was calculated using the grain density data from Table 1. Carbonate content was measured following the "Scheibler" procedure which has a precision of ≤3% (Kenter et al., 1997b). The two standards for dolomite and calcium carbonate were added and checked against the total amount of carbonate. The non-carbonate fraction, or insoluble residue, is mainly organic material and small amounts of quartz. As stated earlier, aluminum oxides are only present in very small weight percentages and, as such, are negligible. The microscopic fabrics were classified according to the system described by Lucia (1995).

Shipboard measurements of physical properties and downhole wireline logging are described in detail by Emeis, Robertson, Richter, et al. (1996). Wireline logging data provided independent values of *P*-wave velocities, porosity, and bulk density. A Long-Spaced Sonic Tool and a Digital Sonic Tool were used to obtain in situ formation velocities at each hole, with a vertical resolution in the range of 0.61 m, assuming that the measurements were free from the effects of formation damage and enlarged bore hole from the drilling. Bulk density measurements were obtained by High-Temperature Lithodensity Tool with a vertical resolution of around 0.45 m. The porosity was derived from a Compensated Neutron Porosity Tool to a vertical resolution also of about 0.45 m. Caliper measurements during logging provided both an indication of hole conditions and key information that was used in correcting logging data (Emeis, Robertson, Richter, et al., 1996). The logging data used in this study were obtained directly from the Borehole Research Group at Lamont-Doherty Earth Observatory, following processing and correction as described in Emeis, Robertson, Richter, et al. (1996; see CD-ROM, back pocket, this volume).

RESULTS

Cross plots of discrete measurements of *P*-wave velocity vs. porosity and density for both holes are shown in Figure 1. Velocities in Hole 966F show a variation of about 1 km/s at a given porosity value and generally follow the trend of the time-average curves by Wyllie et al. (1958) for 4.5 km/s to 7.3 km/s (the matrix velocity of dolomite). However, velocities in Hole 967E plot considerably higher than the time-average equation would predict. The velocity-porosity range of core plugs from the two holes have significantly different ranges that show little overlap. Similarly, cross plots of density vs. velocity show that Hole 966F data scatter around the limestone curve of Gardner et al. (1974), whereas the Hole 967F data lie above this curve (Fig. 1B).

Figure 2A shows that insoluble residue has a clear relationship with sonic velocity for both holes. At insoluble residue values below about 1%-4%, velocities are higher than 3.6 km/s. With increasing in-

Table 1. Summary of index properties and acoustic properties for samples from Sites 966 and 967.

Laboratory number	Core, section, interval (cm)	Depth (mbsf)	Dry density (g/cm^3)	Bulk density (g/cm^3)	Grain density (g/cm^3)	Porosity (fraction)	V_p (km/s)	V_s (km/s)	V_p/V_s	$CaCO_3$ (wt%)	Dolomite (wt%)
	160-966F-										
1	8R-1, 58-62	125.58	2.19	2.37	2.722	0.20	4.797	2.402	1.997	0.97	0.05
2	10R-1, 105-109	145.25	2.33	2.45	2.751	0.15	5.646	2.938	1.922	1.00	0.22
3	10R-2, 37-41	146.07	2.56	2.60	2.757	0.07	5.722	3.022	1.893	1.00	0.26
4	11R-1, 119-122	154.99	2.07	2.30	2.757	0.25	4.349	2.371	1.835	1.05	0.27
5	12R-1, 114-116	164.64	2.39	2.53	2.813	0.15	5.550	3.031	1.831	1.08	0.64
6	12R-1, 117-121	164.67	2.41	2.54	2.873	0.16	5.430	3.035	1.789	1.06	1.05
7	13R-1, 87-91	173.97	1.97	2.22	2.717	0.27	4.078	2.230	1.828	0.99	0.00
8	14R-1, 125-129	183.95	2.37	2.52	2.828	0.16	5.580	3.082	1.811	1.06	0.74
9	15R-1, 4-8	192.44	2.54	2.60	2.838	0.10	6.151	3.117	1.973	1.08	0.81
10	15R-1, 139-143	193.79	2.32	2.49	2.850	0.19	5.359	2.967	1.806	1.08	0.89
11	16R-1, 60-64	202.60	2.26	2.44	2.834	0.20	5.287	2.803	1.886	1.05	0.79
12	16R-2, 44-48	203.93	2.31	2.48	2.853	0.19	5.556	3.060	1.816	1.06	0.91
13	17R-3, 87-91	215.33	2.03	2.30	2.846	0.29	4.623	2.528	1.829	1.07	0.86
14	18R-1, 144-148	222.74	2.13	2.37	2.814	0.24	4.486	2.497	1.797	1.08	0.65
15	19R-2, 125-129	233.63	1.98	2.25	2.762	0.28	3.712	1.857	1.998	1.00	0.30
16	26R-3, 60-64	301.11	1.77	2.04	2.682	0.34	3.066	1.668	1.838	0.63	0.00
17	27R-1, 9-14	307.99	1.60	1.98	2.696	0.41	2.948	1.536	1.919	0.77	0.00
18	28R-2, 56-60	318.68	1.73	2.09	2.708	0.36	3.053	1.578	1.935	0.89	0.00
19	28R-2, 62-65	318.74	1.73	2.08	2.710	0.36	3.252	1.682	1.933	0.92	0.00
20	28R-5, 139-143	323.81	1.83	2.14	2.706	0.32	3.242	1.688	1.921	0.88	0.00
21	30R-1, 78-80	337.58	1.72	2.08	2.708	0.36	3.299	1.682	1.961	0.89	0.00
22	30R-1, 81-85	337.61	1.72	2.07	2.710	0.37	3.103	1.623	1.911	0.92	0.00
23	31R-1, 2-6	346.42	1.95	2.21	2.710	0.28	3.350	1.727	1.940	0.92	0.00
24	31R-3, 43-48	349.65	1.95	2.22	2.709	0.28	3.404	1.786	1.906	0.91	0.00
25	16X-1, 15-21	138.85	1.72	2.07	2.695	0.36	2.418			0.76	0.00
	160-967E-										
26	3R-1, 130-133	130.00	1.72	2.06	2.697	0.36	2.522	1.230	2.051	0.79	0.00
27	4R-2, 111-120	140.89	1.78	2.11	2.707	0.34	2.665	1.304	2.043	0.89	0.00
29	5R-1, 135-140	149.35	1.79	2.12	2.709	0.34	2.963	1.500	1.976	0.91	0.00
30	5R-2, 1-9	149.45	1.80	2.12	2.714	0.34	2.969	1.496	1.985	0.91	0.03
31	5R-3, 1-10	150.91	1.70	2.04	2.708	0.37	2.728	1.458	1.871	0.89	0.00
32	5R-4, 93-103	153.14	1.76	2.09	2.707	0.35	2.847	1.438	1.979	0.88	0.00
33	6R-1, 58-67	158.28	1.81	2.14	2.708	0.33	3.012	1.568	1.921	0.90	0.00
34	6R-2, 34-47	159.51	1.73	2.07	2.709	0.36	2.861	1.555	1.840	0.91	0.00
35	6R-3, 35-40	160.78	1.68	2.04	2.703	0.38	2.709	1.356	1.998	0.85	0.00
36	7R-1, 30-38	167.60	1.66	2.04	2.720	0.39	2.881	1.429	2.015	0.88	0.11
37	8R-1, 21-29	177.11	1.56	1.96	2.696	0.42	2.292			0.78	0.00
38	8R-2, 31-37	178.60	1.66	2.01	2.702	0.39	2.624	1.429	1.836	0.83	0.01
39	9R-1, 95-98	87.45	1.77	2.11	2.715	0.35	3.159	1.619	1.951	0.93	0.03
40	9R-2, 30-33	188.06	1.71	2.03	2.729	0.37	2.919	1.520	1.920	0.91	0.15
41	9R-3, 38-41	189.31	1.67	2.02	2.769	0.40	3.083	1.640	1.880	0.94	0.41
42	10R-1, 120-126	197.40	1.64	2.03	2.757	0.41	2.922	1.501	1.946	0.95	0.31
43	10R-2, 42-49	198.00	1.65	2.04	2.737	0.40	2.917	1.510	1.932	0.93	0.19
44	10R-3, 85-90	199.75	1.65	2.04	2.732	0.40	3.060	1.583	1.932	0.95	0.14
45	11R-1, 60-66	206.40	1.56	1.97	2.710	0.42	2.990	1.531	1.952	0.92	0.00
46	11R-2, 77-82	207.60	1.72	2.07	2.710	0.37	2.994	1.504	1.990	0.92	0.00
47	11R-3, 32-38	208.15	1.65	2.03	2.708	0.39	2.990	1.523	1.963	0.90	0.00
48	12R-1, 81-86	216.21			2.710		3.137			0.92	0.00
49	12R-3, 65-70	218.81	1.65	2.04	2.713	0.39	3.011	1.544	1.949	0.95	0.00
50	13R-1, 129-135	226.39	1.74	2.09	2.715	0.36	3.167	1.623	1.951	0.97	0.00
51	13R-2, 82-88	227.36	1.73	2.08	2.711	0.36	3.089	1.559	1.981	0.93	0.00
52	14R-1, 99-104	235.69	1.72	2.07	2.710	0.37	3.117	1.575	1.980	0.92	0.00
53	14R-2, 37-43	236.57	1.77	2.11	2.713	0.35	3.093	1.584	1.953	0.94	0.00
54	15R-1, 28-36	244.58	1.75	2.10	2.711	0.35	3.011	1.549	1.944	0.93	0.00
55	15R-2, 113-118	246.86	1.71	2.01	2.710	0.37	2.887	1.545	1.869	0.92	0.00
56	16R-1, 52-56	254.42	1.65	1.95	2.711	0.39	2.917	1.636	1.783	0.93	0.00
57	16R-2, 128-133	256.68	1.82	2.15	2.711	0.33	2.989	1.493	2.001	0.92	0.00
58	16R-3, 72-79	257.57	1.72	2.08	2.710	0.37	3.059	1.556	1.967	0.92	0.00
59	17R-1, 70-77	264.20	1.84	2.15	2.710	0.32	3.109	1.602	1.941	0.92	0.00
60	17R-2, 87-92	265.77	1.80	2.13	2.709	0.33	3.019	1.510	1.999	0.91	0.00
61	18R-1, 124-128	274.34	1.85	1.97	2.700	0.32	2.985			0.81	0.00
62	18R-2, 64-70	275.02	1.53	1.95	2.714	0.44	2.919	1.493	1.955	0.96	0.00
63	18R-3, 86-90	276.66	1.68	2.05	2.714	0.38	3.100	1.610	1.925	0.96	0.00
64	19R-1, 108-112	283.78	1.87	2.09	2.708	0.31	3.257			0.90	0.00
65	25R-2, 77-83	342.73	1.85	2.18	2.710	0.32	3.122	1.663	1.877	0.92	0.00
66	28R-1, 85-90	370.15	1.74	2.08	2.711	0.36	3.132	1.658	1.888	0.93	0.00
67	29R-1, 54-59	379.34	2.02	2.24	2.706	0.25	3.356			0.88	0.00
68	32R-1, 30-35	408.00	1.92	2.20	2.715	0.29	3.627	1.918	1.891	0.96	0.00

Notes: V_p = *P*-wave velocity or compressional-wave velocity; V_s = *S*-wave velocity or shear-wave velocity; $CaCO_3$ = carbonate fraction of total weight of sample determined with carbonate bomb; dolomite = dolomite fraction calculated from xrf weight percentages of MgO and CO_3, assuming that no relevant amounts of clays are present (see text for discussion).

soluble residue from about 1%-4% up to 25% (range in insoluble residues for the data set), velocity displays a very gradual, nearly linear, decrease from 3.6 km/s to about 2.5 km/s. Dolomite shows a comparable but inverted and more scattered effect on sonic velocity (Fig. 2B). Samples with dolomite content lower than about 50% have velocities ranging from 2.3 to nearly 6 km/s, whereas samples with dolomite content higher than 50% have velocities between 4.2 and 6 km/s.

Petrographic analyses of thin sections were used to classify the samples in six different groups based on fabric and pore type according to Lucia (1995) and Dunham (1962; Fig. 2C). Two groups (the calcitic grainstone and the calcitic mudstone) are not statistically useful for correlation purposes because they are represented by only one or two samples. The two dolomite groups (dolomite wackestones and mudstones, Lucia's [1995] groups 2.4 and 2.5, respectively) are in agreement with the dolomitic group determined from XRF measure-

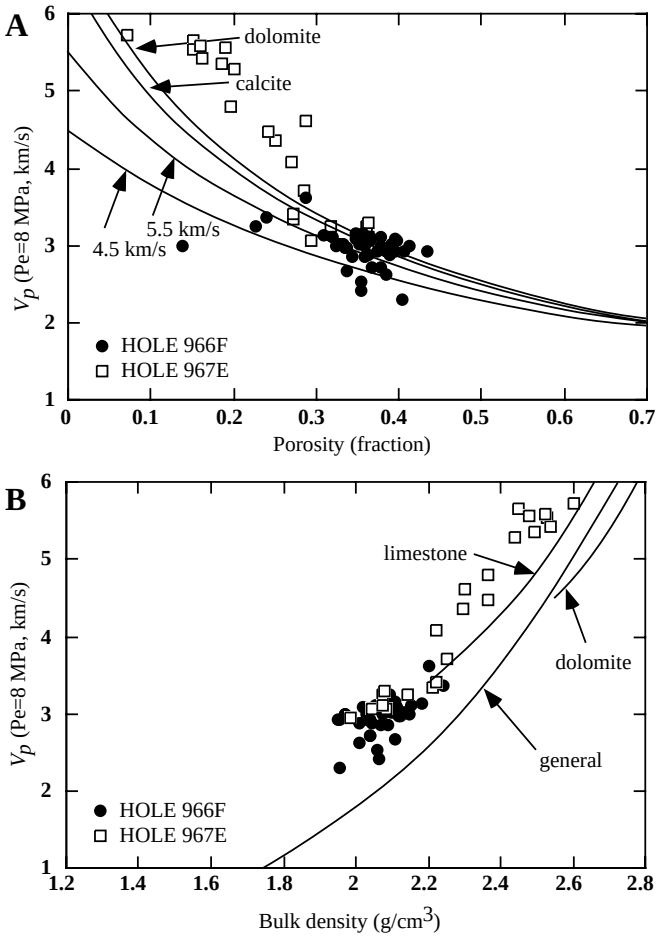

Figure 1. Cross plots of *P*-wave velocity for (**A**) porosity fraction, with Wyllie's time-average equations for dolomite and calcite (Wyllie et al., 1958), and (**B**) bulk density, with curves from Gardner's empirical studies of limestone, dolomite, and shale (Gardner et al., 1974).

ments. They are recrystallized shallow-water rocks with fossil fragments recrystallized to micrite grain size, and rocks with pore spaces that are filled with crystals of sparite up to 100 µm. The calcite groups (mud-dominated packstone and wackestones of Lucia's [1995] groups 3.1 and 3.3, respectively) correspond to the calcite group determined from XRF measurements; they are foraminiferal deep sea sediments with foraminifers up to 450 µm, but they also contain three mixed calcite-dolomite samples. In general, there is no clear relationship between petrographic grouping and sonic velocity. Instead, it seems that mineralogy, variations in insoluble residues, and dolomite content are overprinting the effect of texture and fabric on acoustic behavior of the samples.

The discrete measurements of physical properties as a function of depth in each hole are plotted in Figures 3 and 4 along with the same physical properties determined from the wireline logs. What is most obvious is that the log-derived values and the measured values do not coincide for the upper part of Hole 966F (above about 218 mbsf in Fig. 3) and are offset from each other in Hole 967E, but show similar trends (Fig. 4). The two data sets from the lower section of Hole 966F correspond relatively well. The greatest discrepancies between the wireline data and the laboratory measurements occur where the hole conditions are poorest, as indicated either by large variations in the hole diameter shown by the caliper measurements (given for each hole in Figs. 3, 4) or by the hole diameter exceeding the breadth of the calipers in their most extended condition (e.g., the section be-

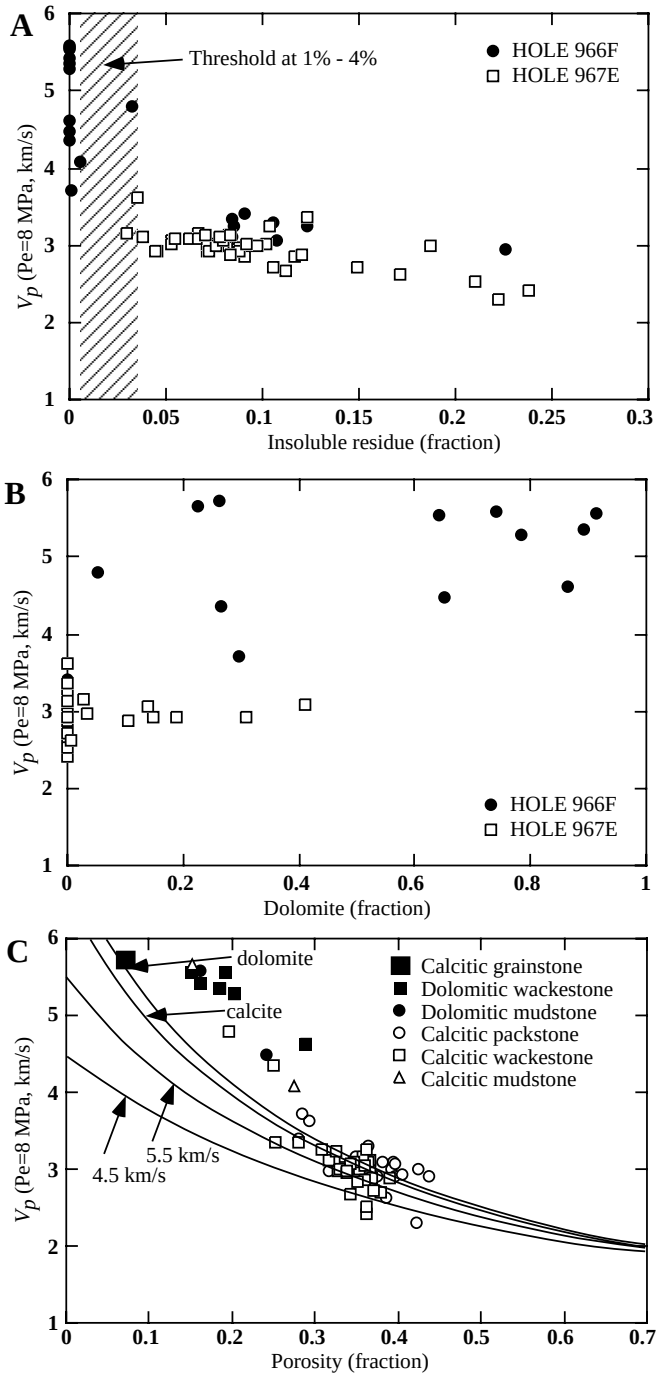

Figure 2. Dependence of *P*-wave velocity on fraction of each sample containing (**A**) insoluble residues, where gray box shows transition zone between insoluble residues, and (**B**) dolomite. The dependence of *P*-wave velocity on porosity fraction for all the samples (**C**) is shown with the rock fabric type indicated according to Lucia's (1995) classification. See text for discussion.

tween 240 and 280 mbsf in Hole 966F, where the Shipboard Scientific Party [1996a] reported very low recovery and the presence of fracturing in the rocks). Where the calipers are wide open there is no guarantee that the sensor pads are against the wall of the hole (see also Paillet and Cheng, 1991).

Strong variability in the hole diameter in the upper part of Hole 966F coincides with the largest discrepancies between the two data

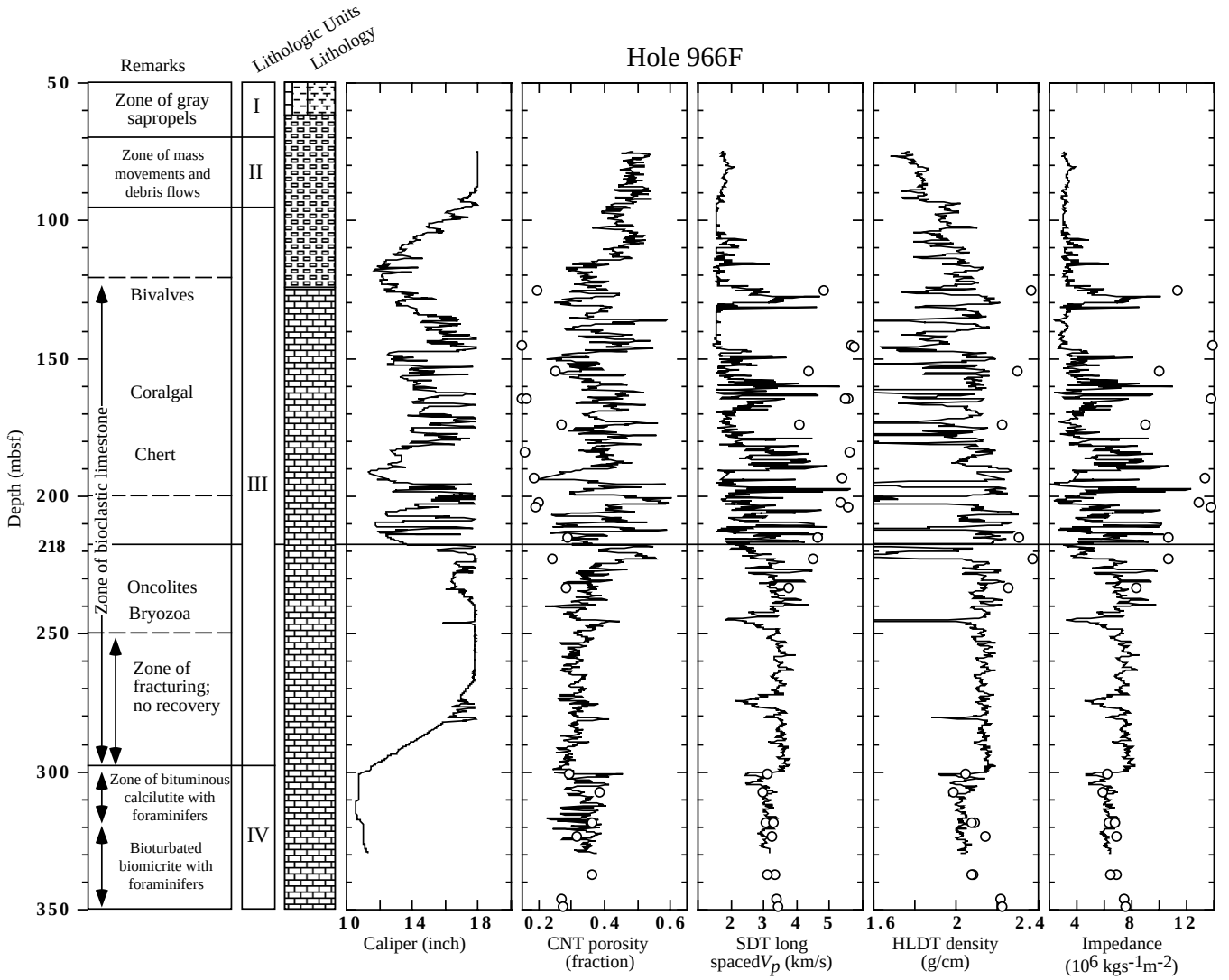

Figure 3. Physical properties of the core plugs (open circles) plotted on the corresponding log-derived downhole variations of the same parameters for Hole 966F (continuous solid lines). Also shown are the general lithology and caliper log on the left. Depths are in meters below seafloor (mbsf). The two intervals indicated by the solid line through all parts of the figure have specific velocity-porosity relationships. See text for discussion.

sets. It is only in the deeper part of the hole (below 300 mbsf in Fig. 3) that the data sets agree, where the caliper reading is around 12 in. Although some spikes in the *P*-wave velocity indicate values as high as the laboratory measurements, there is no correlation between the two. It is clear that in the upper part of the hole there is a lower limit set for the *P*-wave velocities, to which unrealistically low values are set. The spikes in the bulk density are primarily in the opposite direction to the level of the laboratory measurements, which are all ~0.1–0.2 g/cm^3 higher than the wireline log level above 218 mbsf. The neutron porosity is consistently about twice as high as the measured porosities. This difference is nearly two orders of magnitude larger than the estimated error in the laboratory measurements (≤3%).

The caliper log indicates that Hole 967E (Fig. 4) is in much better condition than Hole 966F. There are only a few places where the hole diameter is excessively large and where there are very few large fluctuations in hole diameter downhole. This is reflected in better correlation between the log-derived physical properties and those measured on the core plugs. There is an increasing difference downhole between the neutron porosity and the measured porosity; however, the other plots in Figure 4 show the same trends for both measured and log-derived parameters. Density and *P*-wave velocities derived from the wireline logs are less than the measured values, and the neutron porosity tends to overestimate the laboratory measured porosity.

An important additional way to evaluate the log-derived physical properties in comparison to the measured values is to cross plot various combinations of parameters, which are theoretically related to each other in definable ways. For example, the greater the degree of porosity in a sample, the lower the *P*-wave velocity is expected to be, and the greater the bulk density of a sample, the greater the expected *P*-wave velocity in general. Density and porosity may sometimes be used as a proxy for acoustic velocity. In the cross plots of velocity, density, and porosity that are shown in Figures 5 and 6, there is a very high degree of scatter in the log-derived parameters, as well as crossovers with discrete data and empirical relationships.

The measured velocities, porosities, and densities for Hole 966F samples shown in Figure 5 do not follow closely the empirical curves or discrete measurements also plotted. They do show roughly the same trends, however, except that the decrease in *P*-wave velocity with increasing porosity fraction is greater than that shown by the curves for nearly pure carbonates. Secondly, the log data show a sig-

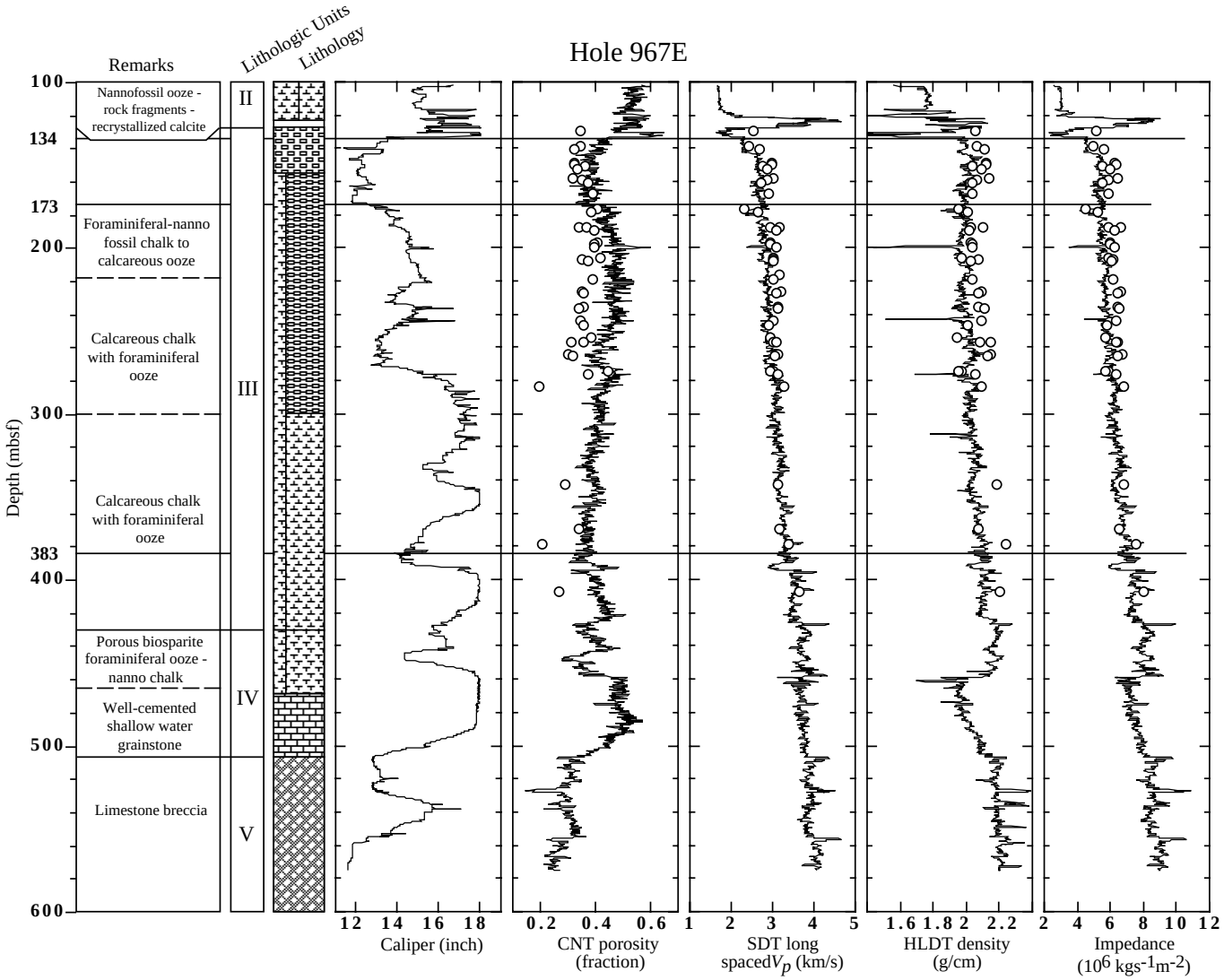

Figure 4. Physical properties of the core plugs (open circles) plotted on the corresponding log-derived downhole variations of the same parameters for Hole 967E (continuous solid lines). Also shown are the general lithology and caliper log on the left. Depths are in meters below seafloor (mbsf). Indicated by the solid lines through all parts of the figure are intervals that have specific velocity-porosity relationships. See text for discussion.

nificant scatter around the discrete data and empirical curves of up to 3 km/s at a given porosity or density. The log-derived values have been plotted in two groups depending on whether they are from above or below 218 mbsf in the hole. The two groups are clearly separated in Figure 5. The data from the upper part of the hole show no obvious relationship between either neutron porosity or bulk density and *P*-wave velocity. The data from the lower part of the hole plot closer to the measured data and the curves, but the porosity data form a cloud of data points that show only a very vague correlation with the relationship shown between the discrete measurements of *P*-wave velocities and porosity. Moreover, the trend of the main cloud of bulk density data seems to be different from that shown by the discrete measurements or from the curves based on fundamental physical relationships (Bourbié et al., 1987). Discrete measurements of density and porosity show, as expected, a linear relationship that intersects the y-axis at about 2.82 g/cm^3, the density at zero porosity of nearly pure dolomite (Fig. 5C). The wireline logging data, however, show a large scatter and a trend that crosses that of the discrete measurements.

The cross plots of data from Hole 967E in Figure 6 differ from those of Hole 966F in that the data are less scattered and show more pronounced trends. The discrete values of *P*-wave velocities, porosities, and bulk densities plot very closely to the empirical curves for carbonates. The log-derived values have been subdivided on the basis of downhole depth, and plot in rather distinct groups that each cross the trends of the discrete data and empirical curves. The uppermost group (100–134 mbsf) shows considerable scatter in *P*-wave velocity and bulk density values. The second group downhole (134–173 mbsf) plots in almost the same place as the discrete measurements, and can be seen from Figure 4 to represent that part of the hole that is inferred from the low caliper values to be in the best condition. The third group downhole (173–383 mbsf) shows considerable scatter in bulk density but reasonable grouping in the neutron porosity cross plot with *P*-wave velocity, except that the values lie consistently above the discrete measurements and curves (as indicated also in Figure 4). In comparison to the curves and the discrete measurements the deepest group (383–578 mbsf) shows anomalously high *P*-wave velocity, the neutron porosity seems to be too high, and the density too

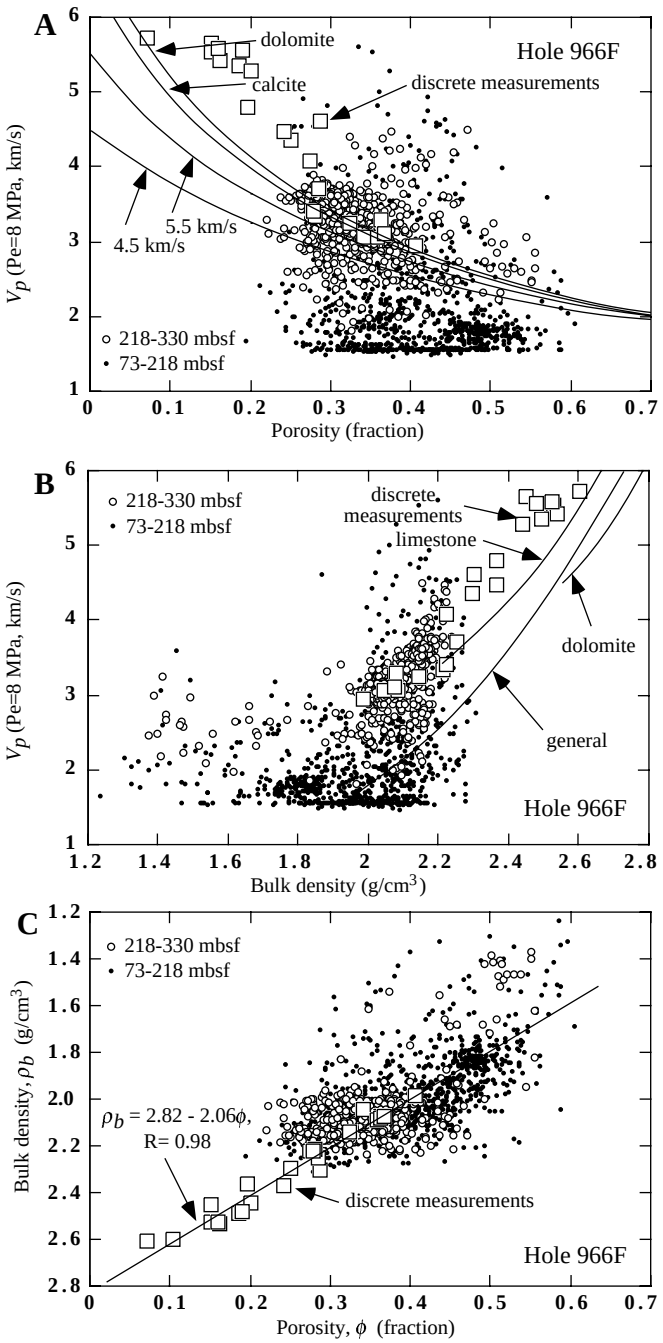

Figure 5. Cross plots of *P*-wave velocity for (**A**) porosity, (**B**) bulk density, and (**C**) bulk density plotted against porosity, for different intervals in Hole 966F. Discrete measurements are shown as large open squares, and the log-derived values are plotted according to their depth range below seafloor. Also shown are Wyllie's curves in (A) and Gardner's curves in (B). The straight line in (C) is the best fit through the data, with the coefficient of correlation given as R. Note that the log-derived porosity-velocity relationships for the various intervals (indicated in Fig. 3) each have a different trend, and all deviate from the discrete data and general velocity transforms. See text for discussion.

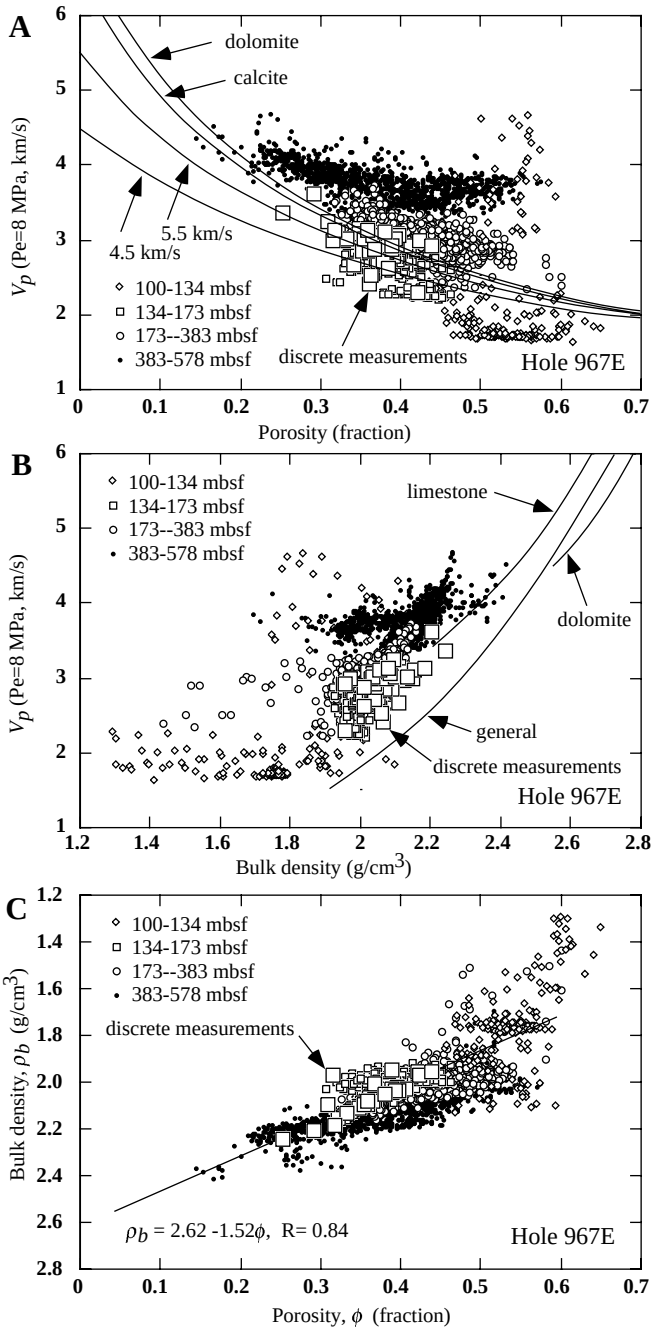

Figure 6. Cross plots of *P*-wave velocity for (**A**) porosity, (**B**) bulk density, and (**C**) bulk density plotted against porosity, for different intervals in Hole 967E. Discrete measurements are shown as large open squares, and the log-derived values are plotted according to their depth range below seafloor. Also shown are Wyllie's curves in (A) and Gardner's curves in (B). The straight line in (C) is the best fit through the data, with the coefficient of correlation given as R. Note that the log-derived porosity-velocity relationships for the various intervals (indicated in Figure 4) each have a different trend, and all deviate from the discrete data and general velocity transforms. See text for discussion.

low. Similarly, density-porosity relationships cross those of discrete measurements and their trends would suggest deviations of 2.1 to 2.3 g/cm^3 at zero porosity for nearly pure carbonate (Fig. 6C).

DISCUSSION

The controls on the acoustic properties of carbonate rocks, in order of significance, are porosity, insoluble residue, and dolomite content. In general the Hole 966F data follow the time-average equation by Wyllie et al. (1958) and the limestone curve by Gardner et al. (1974). The relationships are very similar to published data of nearly pure carbonates (e.g., Anselmetti and Eberli, 1993; Anselmetti, 1994; Kenter and Ivanov, 1995). The negative effect of insoluble residue on the acoustic velocities of carbonates has earlier been documented by King et al. (1992) and Stafleu et al. (1994). Careful study of the different dolomite textures shows that the most common is dolomite replacement after calcite: in other words, mimetic dolomite cement. According to recent findings by F.S. Anselmetti (pers. comm., 1997) and published work by Anselmetti (1994), the mimetic dolomite maintains velocities that, at given porosities, are even higher than the matrix velocity of the dolomite crystal (~7.2 km/s at 0% porosity).

In general, the time-average equation of Wyllie et al. (1958) and the empirical limestone equation by Gardner et al. (1974) fail to explain the variation of *P*-wave velocity at a given porosity value but the laboratory data do show a similar trend. Whether from wireline logs or discrete laboratory measurements, it is expected that velocity, porosity, and density interrelationships remain similar. The wireline logging data, however, show excessive scatter and, for certain intervals, trends that cross those present in the discrete data and those known from the literature (e.g., Wyllie et al., 1958; Gardner et al., 1974; Rafavich et al., 1984; Anselmetti and Eberli, 1993; Kenter and Ivanov, 1995; Kenter et al., 1997b) The scatter present along the general trends of velocity-porosity and velocity-density transforms can be attributed to the effect of parameters like mineralogy, cement type, pore type, and so on. Extrinsic parameters like pressure and temperature will certainly have an effect on the variation along these trends but not change the orientation of the trend. This is similar to the better documented relationships in siliciclastic systems.

In all of the figures and the table, the measured values should be considered to be accurate representations of the downhole variations of physical properties from discrete samples of the different formations because the laboratory conditions approximate the in situ conditions of the samples. The values obtained from the wireline logs are dependent on hole conditions, the calculations that transform the logged data into the acoustic parameters (including the corrections that compensate for variations in the hole condition), and sensitivity and resolution of the tools, regardless of the skill of the loggers. Under poor hole conditions it can be expected that the wireline data may show low *P*-wave velocities and density and high neutron porosity (Theys, 1991; Paillet and Cheng, 1991; Bourbié et al., 1987). The wireline data used here from Holes 966F and 967E vary in quality from good to very poor, with more poor data than good data. Other factors that may bias or affect the comparison between discrete data and log data are different scales, acoustic frequencies, and measuring distances. For example, the sonic tool averages velocities over ~60 cm and therefore "smooths" thin alternations of high and low velocities toward lower log velocities. Finally, the presence of a borehole is a physical discontinuity of the petrophysical properties of the formation (Bourbié et al., 1987). It is apparent that post-logging corrections to the data (already applied to these data) may locally shift some unrealistic relationships to more physically accepted values (e.g., unrealistically low velocities shifted up to 1.550 km/s), but the corrections do not necessarily render the data consistent with the documented velocity transforms for the given rock formations.

Based on the caliper data the wireline data plotted in Figure 3 are clearly of poor quality in the upper section of the hole, above 218 mbsf (and possibly from above 290 mbsf). The discrete data show a certain variability also, suggesting that a variable lithology may be one of the reasons for the variability in the condition of the hole in the upper section. Figure 5 shows that there is a group of high *P*-wave velocity samples from Hole 966F that does not fit Wyllie's curves. Figure 2 indicates that the reasons for this are that the upper part of Hole 966F contains nearly pure carbonate of which a very high percentage is dolomite with a moldic, vuggy pore type, in terms of Lucia's (1995) classification. Downhole, the dolomitic wackestones give way to calcitic carbonates that plot closer to the curves derived by Wyllie et al. (1958). Thus, the apparent discrepancy in trend of the data with respect to the curves could be seen as a result of two populations of data that are simply separated from each other by a slight shift in *P*-wave velocity near a porosity value of 0.25 to 0.30.

The scatter of wireline data and lack of a well-defined relationship of *P*-wave velocity to either bulk density of neutron porosity in Figure 5 confirms the poor quality of the log-derived data for Hole 966F. The data from the upper part of the hole form a cluster near the low velocity limit, almost regardless of density and porosity variations. It is assumed that corrections to the velocity logs (e.g., for transit time stretching or cycle skipping when the signal is weak [Serra, 1984]) are responsible for the abnormal clusters because of the large scatter of data. The data from deeper samples exhibit a similar scatter, but plot in roughly the expected part of the graph. Nevertheless, it is not possible to separate out the correct from the incorrect values within this cloud.

Figure 6 displays a different type of noise. The wireline data for Hole 967E are separated into distinct populations by depth. The shallowest data are probably incorrect because of bad hole conditions, as indicated by the caliper plot in Figure 4; and they plot in a similar manner to shallow data in Hole 966F. The data from the deepest section of the hole show too high a porosity for the given velocity range. This can be explained by noting that the neutron porosity variations below 383 mbsf in Figure 4 are not only directly correlated with the caliper log but also are consistently higher than those for the section above (which is possible, but in this case improbable). It appears that the deep data could be 'corrected' by shifting them into a lower porosity region of Figure 6A (or a higher density region of Figure 6B), but the trend would not be corrected and the amount of shifting would be arbitrary. Thus, although the wireline data from Hole 967E appear to be somewhat reasonable in Figure 4, it is clear from Figure 6 that they are probably much worse than Figure 4 would suggest, and that simple corrections are not to be found.

The samples used for discrete measurements in Hole 967E were obtained mainly from the section between 134 mbsf and 300 mbsf, where Figure 4 shows that the hole conditions are probably good. The wireline data from this part of the hole largely coincide with the discrete measurements except that the neutron porosities tend to be slightly too high and some of the bulk densities are anomalously low. The samples used for discrete measurements, therefore, can be seen to be representative of only a small part of the hole—less than one third. Hole 966F is poorly represented by samples also because the sampling interval is greater in the upper half of the hole and in the lowest 30 m than in the sampled part of Hole 967E.

One impetus for this study was the desire to use the discrete measurements to 'calibrate' the logging data and then to use the combined data set to make synthetic seismograms. The synthetic seismograms are useful both for linking important seismic reflectors with the geologic source for better interpretation of seismic profiles, and for studying the physical causes of seismic reflections in general. That means that they should be based on an accurate model of the physical properties variations downhole. During this study, synthetic seismograms that were based on acoustic impedance logs derived from the wireline data (uncorrected by the ground truth data), showed some similarities with site survey seismic profiles. The research reported here demonstrates that correlation of such synthetic seismograms with seismic profiles is fortuitous rather than real. Perhaps the acoustic impedance variations do match some of the more significant geological variations that are expected in the holes, because it is the

changes in these parameters rather than their absolute values that are more important; however, the very high level of noise, or variability, in the logs for the holes makes it unlikely that the geological variations could be well-modeled by noisy acoustic impedance variations. Therefore, although the synthetic seismograms might look correct, geological inferences from them would be wrong.

It is also unlikely that the discrete measurements reported here can be used to improve or correct the wireline data from the two holes studied to the point where the logs would be acceptable for synthetic seismograms. Downhole diversity in lithology, porosity, and degree of consolidation is responsible not only for the variability in the acoustic properties, but also for the varying hole conditions and core recovery. Without being able to correct for missing sections the exercise is futile. This is true even of Hole 967E where the lithology is thought to be relatively monotonous from the apparent lack of large fluctuations downhole in the well-log data as well as from the core descriptions and petrographic observations (Shipboard Scientific Party, 1996b). Simply shifting the level of the wireline data, as is suggested from Figure 4, would only shift the large volume of noise that is present, as shown in Figure 6. Continuing research will examine the possibility of characterizing acoustic properties downhole for sampled units definable, for example, in the Formation Micro-Scanner (FMS) logs. If there is a correlation between sampled units and distinct units determined from other logs like FMS, then it may be possible to assign acoustic properties to the discrete units and reduce the noise level in the log-derived parameters by using discrete values in units where wireline logs are noisy.

CONCLUSIONS

Careful comparison between discrete measurements (68 core plugs) of acoustic properties, general velocity transforms, and logging data from Holes 966F and 967E from ODP leg 160, resulted in the following conclusions.

Discrete measurement of acoustic properties indicate that *P*-wave velocities are controlled, in order of significance, by porosity, insoluble residue, and type of dolomite. Insoluble residues below 1%–4% do not affect velocity, but contents higher than this threshold have a negative, nearly linear effect on sonic velocity. Some types of replacement dolomite, here mimetic, can produce higher sonic velocities than predicted by the time-average equation for similar porosities.

The wireline logs underestimate the velocities and densities and overestimate the porosities in Holes 966F and 967E. One of the main reasons is poor hole conditions, expressed by deviations in the width of the hole and resulting in poor contact between the tools and sides of the holes. Other reasons are upscaling effects of frequency and distance. Corrections made to the logs may add noise, even though they may improve the values in some cases. However, the corrections do not result in data that are consistent with the generally accepted velocity transforms for given rock formations.

It would be dangerous to try to correct the wireline logging data only on the basis of a small set (68) of possibly unrepresentative samples. Moreover it would be dangerous to make synthetic seismograms either with the log-derived acoustic parameters or with the measurements from the samples alone. Determining the downhole variations in acoustic properties must follow from a more careful analysis of other logging data, general velocity transforms for the given lithologies, and, ideally, an extensive database of discrete measurements on core plugs for ground truth measurements.

ACKNOWLEDGMENTS

One of the authors (Woodside) thanks the Netherlands Foundation for Geosciences (Stichting GOA) for financial support for participation on ODP Leg 160. We wish to thank Nanda Rave-Koot and Volker Wiederhold for their assistance in preparing the rock plugs. Marianne Broekema and Ed Verdurmen are acknowledged for XRF analyses. The ultrasonic equipment was engineered by Carl Coyner and benefited from rapid and successful electronic first-aid by Johan de Lange. Funding to the second author was provided through the Industrial Associates Program of Wolfgang Schlager. The analysis reported here is a part of Köhnen's undergraduate thesis work. This research is a contribution to ongoing research on the geological/physical sources of seismic reflections carried out at the Free University in Amsterdam.

REFERENCES

Anselmetti, F.S., 1994. Physical properties and seismic response of carbonate sediments and rocks [Ph.D. thesis]. ETH Geol. Inst.

Anselmetti, F.S., and Eberli, G.P., 1993. Controls on sonic velocity in carbonates. *Pure Appl. Geophys.*, 141:287–323.

Bourbié, T., Coussy, O., and Zinszner, B., 1987. *Acoustics of Porous Media:* Paris (Ed. Technip.).

Dunham, R.J., 1962. Classification of carbonate rocks according to depositional texture. *In* Ham, W.E. (Ed.), *Classification of Carbonate Rocks.* AAPG Mem., 108–121.

Emeis, K.-C., Robertson, A.H.F., Richter, C., et al., 1996. *Proc. ODP, Init. Repts.*, 160: College Station, TX (Ocean Drilling Program).

Gardner, G.H.F., Gardner, L.W., and Gregory, A.R., 1974. Formation velocity and density: the diagnostic basics for stratigraphic traps. *Geophysics*, 39:770–780.

Kenter, J.A.M., Fouke, B.W., and Reinders, M., 1997a. Effects of differential cementation on the sonic velocities of Late Cretaceous skeletal grainstones (Southeastern Netherlands). *J. Sediment. Res.*, 67:178–185.

Kenter, J.A.M., and Ivanov, M., 1995. Parameters controlling acoustic properties of carbonate and volcaniclastic sediments at Sites 866 and 869. *In* Winterer, E.L., Sager, W.W., Firth, J.V., and Sinton, J.M. (Eds.), *Proc. ODP, Sci. Results*, 143: College Station, TX (Ocean Drilling Program), 287–303.

Kenter, J.A.M., Podladchikov, F.F., Reinders, M., van der Gaast, S., Fouke, B.W., and Sonnenfeld, M.D., 1997b. Parameters controlling sonic velocities in a mixed carbonate-siliciclastics Permian shelf-margin (upper San Andres Formation, Last Chance Canyon, New Mexico). *Geophysics*, 62:1–16.

King, M.S., Shams-Kanshir, M., and Worthington, M.H., 1992. Witchester seismic cross-hole test site: petrophysics studies of core. *Int. Conf. Offshore Oil and Gas Field Prosp., Moscow.*

Lucia, F.J., 1995. Rock-fabric/petrophysical classification of carbonate pore space for reservoir characterization. *AAPG Bull.*, 79:1275–1300.

Paillet, F.L., and Cheng, C.H., 1991. *Acoustic Waves in Boreholes:* Boca Raton, FL (CRC Press).

Rafavich, F., Kendall, C.H.St.C., and Todd, T.P., 1984. The relationship between acoustic properties and the petrographic character of carbonate rocks. *Geophysics*, 49:1622–1636.

Reeder, R.J. (Ed.), 1983. *Carbonates: Mineralogy and Chemistry.* Rev. Mineral., 11:1–399.

Serra, O., 1984. *Fundamentals of Well-Log Interpretation* (Vol. 1): *The Acquisition of Logging Data:* Dev. Pet. Sci., 15A: Amsterdam (Elsevier).

Shipboard Scientific Party, 1996a. Site 966. *In* Emeis, K.-C., Robertson, A.H.F., Richter, C., et al., *Proc. ODP, Init. Repts.*, 160: College Station, TX (Ocean Drilling Program), 155–213.

————, 1996b. Site 967. *In* Emeis, K.-C., Robertson, A.H.F., Richter, C., et al., *Proc. ODP, Init. Repts.*, 160: College Station, TX (Ocean Drilling Program), 215–287.

Stafleu, J., Everts, A.J.W., and Kenter, J.A.M., 1994. Seismic models of a prograding carbonate platform: Vercors, South-east France. *Mar. Pet. Geol.*, 16:517–537.

Theys, P.P., 1991. *Log Data Acquisition and Quality Control:* Paris (Ed. Technip).

Wyllie, M.R.J., Gregory, A.R., and Gardner, G.H.F., 1958. An experimental investigation of factors affecting elastic wave velocities in porous media. *Geophysics*, 23:400.

Date of initial receipt: 14 February 1997
Date of acceptance: 31 October 1997
Ms 160SR-032